Surgery Article

HAND
1–8

DOI: 10.1177/1558944719831341
hand.sagepub.com

A Biomechanical Comparison of Fiberglass Casts and 3-Dimensional–Printed, Open-Latticed, Ventilated Casts

Paul Hoogervorst[1], Riley Knox[1], Kara Tanaka[1], Zachary M. Working[1], Ashraf N. El Naga[1], Safa Herfat[1,2], and Nicolas Lee[1]

Abstract

Background: The aim of this study was to quantify the stabilizing properties of a 3-dimensional (3D)-printed short-arm cast and compare those properties with traditional fiberglass casts in a cadaveric subacute distal radius fracture model. **Methods:** A cadaveric subacute fracture model was created in 8 pairs of forearms. The specimens were equally allocated to a fiberglass cast or 3D-printed cast group. All specimens were subjected to 3 biomechanical testing modalities simulating daily life use: flexion and extension of digits, pronation and supination of the hand, and 3-point bending. Between each loading modality, radiological evaluation of the specimens was performed to evaluate possible interval displacement. Interfragmentary motion was quantified using a 3D motion-tracking system. **Results:** Radiographic assessment did not reveal statistically significant differences in radiographic parameters between the 2 groups before and after biomechanical testing. A statistically significant difference in interfragmentary motion was calculated with the 3-point bending test, with a mean difference of 0.44 ($\pm$0.48) mm of motion. **Conclusions:** A statistically significant difference in interfragmentary motion between the 2 casting groups was only identified in 3-point bending. However, the clinical relevance of this motion remains unclear as the absolute motion is less than 1 mm. The results of this study show noninferiority of the 3D-printed casts compared with the traditional fiberglass casts in immobilizing a subacute distal radius fracture model. These results support the execution of a prospective randomized clinical trial comparing both casting techniques.

Keywords: 3D printing, additive manufacturing, biomechanics, distal radius, fracture cast

Background

Distal radius fractures are common, with an incidence of 254 to 278 per 100 000 person-years.[1,2] The indications for operative and nonoperative management of these fractures are still subject to debate. Recent systematic reviews and meta-analysis show little difference between the 2 options.[3,4] In the past few decades, there have been minimal advances and few reports on materials used for nonoperative treatment of distal radius fractures.[5-8] The primary emphasis has been on optimizing operative treatment of these fractures by means of optimizing surgical techniques, fracture-specific plates, and rehabilitation protocols.

Nonoperative management of distal radius fractures typically includes an early period of wrist and elbow immobilization by means of either a sugar-tong splint or a long-arm cast followed by transition to a short-arm cast. In our experience, the transition time to a short-arm cast varies among practices. The rationale for a short-arm cast is that with early callus formation and fracture consolidation, limited forearm pronation and supination is tolerated and elbow motion is allowed. Nonoperatively treated distal radius fractures are most often immobilized in a fiberglass cast.

The drawback of a cast is that patients often complain that it is cumbersome, irritating, and malodorous, and that it interferes with personal hygiene. This is especially problematic with injuries that require prolonged immobilization, such as scaphoid fractures.

An emphasis on patient satisfaction has gained more importance recently in the wake of patient-centered reform in health care. New developments in 3-dimensional (3D) printing make it possible to fabricate a patient-specific cast to immobilize the fractured distal radius. These casts use an open-lattice, ventilated design

[1]UCSF/ZSFG Orthopaedic Trauma Institute, San Francisco, CA, USA
[2]Médecins Sans Frontières (MSF) Foundation, Paris, France

Corresponding Author:
Paul Hoogervorst, UCSF/ZSFG Orthopaedic Trauma Institute, 2550 23rd Street, San Francisco, CA 94110, USA.
Email: paul.hoogervorst@ucsf.edu

Figure 1. Example of a 3-dimensional–printed cast.

that is customized to the individual patient and is anatomically accurate (Figure 1).

The patient-specific anatomic scans can easily be obtained with a handheld 3D infrared scanner (Structure Sensor; Occipital, Inc., San Francisco, California). The recyclable nylon material is lighter and waterproof so that patients can bathe and shower with it, which may potentially improve patient satisfaction while maintaining the same immobilizing qualities.

Although 3D-printed casts (3DPC) are Food and Drug Administration exempt and are now commercially available, evaluation of their fracture-stabilizing properties before widespread application of this innovative technology is necessary.

To date, there are neither biomechanical studies available evaluating 3D-printed short-arm casts nor studies comparing them with traditional fiberglass casts in patients with distal radius fractures.

The aims of this study were to quantify the stabilizing properties of a 3D-printed short-arm cast and to compare those properties with traditional fiberglass casts in a cadaveric subacute distal radius fracture model.

Materials and Methods

Sixteen cadaveric forearms from 8 individuals (4 men, 4 women, age: 60.6 $\pm$ 6.1 years) were used. None of the specimens had any recorded surgical history, relevant trauma to the forearm determined by radiographic screening, or diseases that affected bone metabolism. The number of specimens evaluated was deemed sufficient based on the study by Santoni et al[9] which compared a thermoformable bracing system with fiberglass casts and calculated that 5 specimens are sufficient to make an adequate biomechanical comparison. Because the study was an in vitro cadaveric study, at our institution institutional review board approval was not required.

Specimen Preparation

Screening, radiographic evaluation, and measurements of all specimens included radial height, inclination, and volar tilt. The superficialis and profundus flexor tendons of all specimens were bundled using FiberWire (Arthrex, Naples, Florida). A 1-cm dorsal wedge osteotomy was performed through a dorsal approach starting from the proximal end of Lister's tubercle and leaving a small portion of the volar cortex intact. Resection of the radial and ulnar cortices of the radius was fluoroscopically confirmed to ensure that indeed only a small portion of the volar cortex remained. It was ascertained that all prepared specimens exhibited motion of the fracture elements under low forces without immobilization under fluoroscopy. The volar cortex was left partially intact to simulate a partially healed distal radius fracture, with early callus formation often seen at 2 to 3 weeks after injury, the time point in which a clinical transition to a short-arm cast would take place at our institution. Eight specimens (4 left/4 right) were casted using 2 rolls of 4-in cotton padding and 2 rolls of 4-in fiberglass cast (Delta-Lite Plus; BSN Medical, Inc., Charlotte, North Carolina). A dorsal 1-in $\times$ 3-in window was created in the casts through which 2.0 mm Kirschner wires (K-wires) were bicortically inserted into the distal and proximal fragments to serve as anchoring points for the 3D motion-tracking sensors (3020

Figure 2. Mechanical testing setup: (a) flexion-extension, (b) pronation-supination, and (c) 3-point bending.

Optotrak; NDI, Waterloo, Canada). These motion sensors were placed as close as possible to the fracture without interfering with the cast itself. Eight specimens were casted using a 3DPC (Standard Cyborg, San Francisco, California). These specimens were scanned using the handheld 3D infrared Structure Sensor (Occipital, Inc.). The casts were designed using proprietary Standard Cyborg software and printed from HP PA12 Nylon using an HP Multi Jet Fusion Printer (Palo Alto, California). The 3DPCs were designed with an open lattice including a dorsal window to accommodate the bicortical anchoring K-wires and the motion-tracking sensors in both the proximal and distal fragments. After specimen preparation, radiological evaluation was repeated to evaluate for possible fracture displacement.

Mechanical Testing Setup

All specimens were tested in a standardized order. Three loading protocols were used to simulate activities of daily living: flexion and extension of digits, pronation and supination of the hand, and 3-point bending of the construct. Radiographs were taken between each loading modality to evaluate for possible interval displacement.

For flexion-extension testing, the specimens were vertically positioned on a custom-made jig which allowed finger flexion and extension (Figure 2a).

The 3D motion-tracking sensors attached to the K-wires embedded in the fracture element fragments were placed through a window in the supporting board. Fishhooks with fishing line were placed on the second to fifth fingertips. The lines were bundled and threaded through a pulley wheel.

Weights (1.8 kg) were attached to the end of the bundled line to ensure finger extension. The FiberWire, used for bundling of the flexor tendons, was secured to the base of the servo-hydraulic press (Mini Bionix; MTS, Eden Prairie, Minnesota) to create flexion of the fingers.

The pronation and supination of the hand was tested using the multi-axis jig attached to the MTS load cell plate. A clamping fixture was attached to the MTS actuator to secure the hand.

The K-wires were drilled through the distal metacarpals and attached to the clamp (Figure 2b). Immobilization of the cast was ensured.

The 3-point bending tests were set up by attaching 2 fulcrum supports to MTS load cell plate and 1 fulcrum support to the MTS actuator. The bottom support fulcrums contacted the volar surface of the cast and were positioned 3 cm from the volar edge of the cast. The top fulcrum contacted the center of the cast, and it was ascertained that it did not coincide with the fracture gap or K-wire placement (Figure 2c).

Loading Protocols

The loading protocols were based on a combination of previously published force parameters[10] and the prestudy testing of the failure of a fiberglass cast during 3-point bending:

1. *Flexion and extension of the fingers* was achieved by applying 1000 loading cycles (20-100 N tensile force) to the flexor tendon bundle at 0.5 Hz.
2. *Pronation and supination of the hand* was achieved by applying 1000 cycles of torque (−0.5 to 0.5 N m) to the hand/wrist at 0.5 Hz.

3. *Three-point bending* of the construct was applied for 1000 cycles (50-500 N) at 0.5 Hz.

Radiographic Evaluation

At the start of the study and after each biomechanical testing modality, the specimens were evaluated fluoroscopically in anteroposterior (AP) and lateral views. All images were calibrated using a 5-mm-diameter metal spherical marker as a measurement reference. Radial inclination, radial height (in millimeter), volar tilt, and fracture gap (in millimeter) on both the AP and lateral views were measured. Measurements were performed in random order by an independent observer using ImageJ (www.imagej.net, National Institutes of Health), an open-source image processing program designed for scientific multidimensional images. Before measurements were performed, a training session was conducted. The first 15 measurements were repeated to prevent measurement errors during the learning curve.

Fracture Motion Analysis

Motion of the fracture elements was recorded at 100 Hz throughout all testing. The fracture motion is detected by the movement (mm) of Optotrak sensors on opposite sides of the fracture in relation to each other at the last cycle of each testing regimen.

Statistical Analysis

A pairwise statistical analysis was performed. Each 3DPC specimen was compared with its contralateral fiberglass cast specimen. For all parameters, normality was assessed using the Shapiro-Wilk test. Statistical differences for both the radiological measurements and fracture motion between the groups were determined using the paired Student *t* test or the Wilcoxon signed rank test depending on the normality of distribution (IBM SPSS Statistics, version 24). A P value of $<.05$ was considered statistically significant.

Results

Specimen Data

The characteristics of the specimens are shown in Table 1.

Table 1. Specimen Characteristics.

Specimen	3DPC	FC	Sex	Age	Weight, kg
1	L	R	F	59	52
2	L	R	M	72	77
3	L	R	M	61	93
4	L	R	F	59	113
5	R	L	F	60	88
6	R	L	F	66	59
7	R	L	M	52	75
8	R	L	M	56	104

Note. 3DPC = 3D-printed cast; FC = fiberglass cast; L = left; R = right; F = female; M = male.

Radiographic Outcomes

Figure 3 illustrates the measurement results of the radiographic parameters before the start of the biomechanical testing and after each sequential testing modality. Results of radial height, inclination, and fracture gap length measured on the lateral projection exhibited little variation compared with the volar tilt and fracture gap length on the AP projection (Figure 3). However, the absolute change in measured differences remained small in both casting groups before and after all 3 testing cycles in all measured radiographic parameters.

Table 2 reports the results of the statistical analysis for differences in radiological outcomes between the 2 casting groups. Using the Shapiro-Wilk test, normality was assessed. No statistically significant differences were calculated between specimens casted in a traditional cast versus those in a 3DPC when comparing the mean difference for the radiological measurements at the start of biomechanical testing and after all testing was completed.

Fracture Motion

The fracture motion at the last cycle of each testing modality (flexion-extension, pronation-supination, 3-point bending) was recorded (Figure 4). Motion of the fracture elements in relation to each other during the flexion-extension testing ranged from 0.03 to 0.89 mm and 0.09 to 1.09 mm for the traditional casts and the 3DPCs, respectively. Motion during the pronation-supination testing ranged from 0.04 to 3.48 mm and 0.07 to 2.22 mm for the traditional casts and the 3DPCs, respectively. Motion during the 3-point bending test ranged from 0.01 to 0.83 mm and 0.02 to 2.1 mm for the traditional casts and the 3DPCs, respectively.

The smallest specimens (1 and 6) showed more interfragmentary motion than the other specimens.

The mean difference between the pairs and standard deviation (SD) is displayed in Table 3. The paired Student *t* test was used, and no statistically significant differences were calculated between specimens casted in a traditional cast versus the 3DPC for the flexion-extension and the pronation-supination testing.

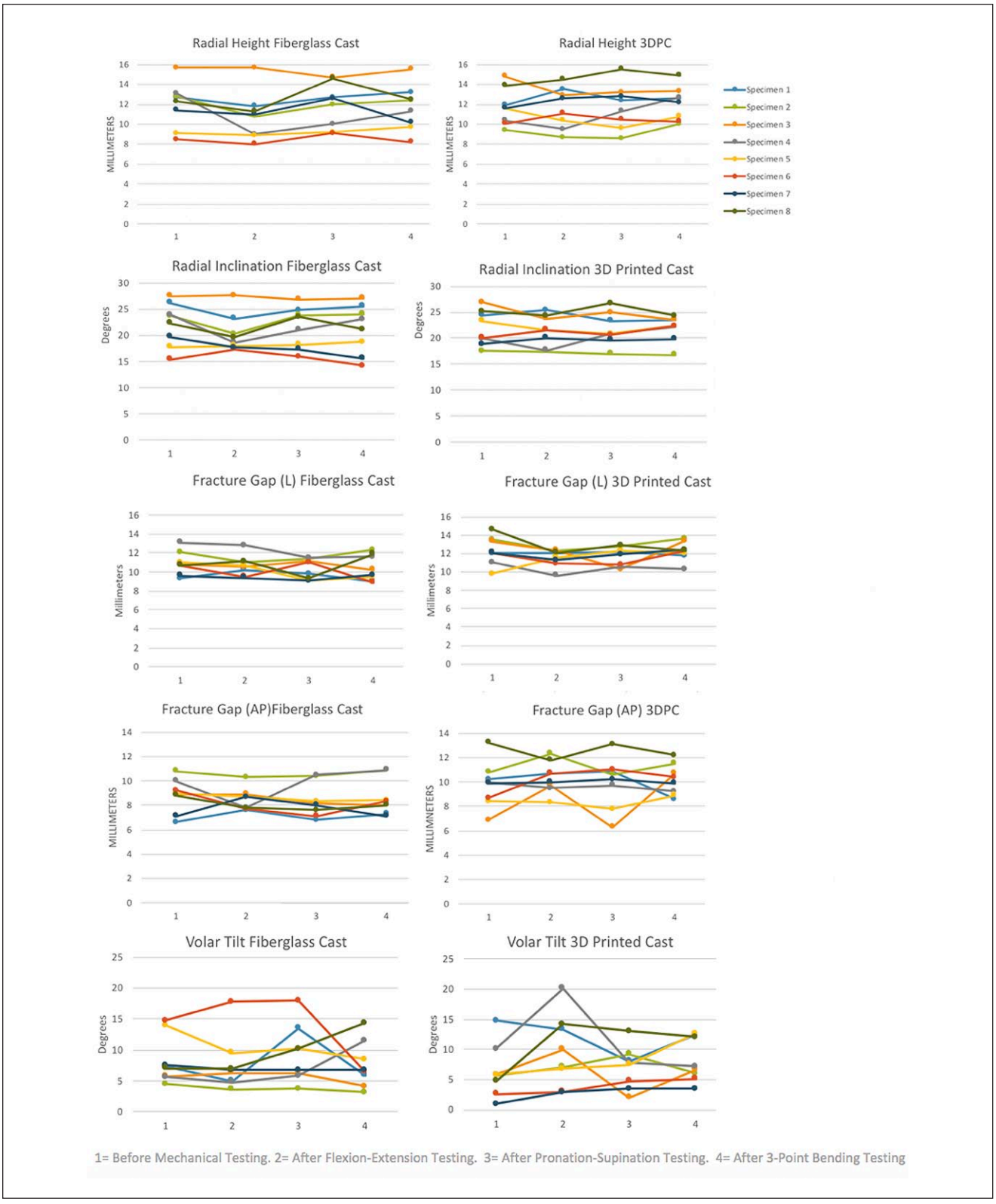

Figure 3. Results of the radiographic parameters before and after each subsequent biomechanical testing modality.
Note. 3DPC = 3D-printed cast; AP = anteroposterior; L = lateral.

Table 2. Results of Measurements and Statistical Analysis for Difference Between Initial and Final Testing Radiographic Parameters.

Measurement	Mean difference	SD	95% CI	*P* value
Radial inclination, deg	0.700	2.901	−1.725 to 3.123	.517
Radial height, mm	0.713	1.755	−0.755 to 2.180	.289
Fracture gap anteroposteriorly, mm	0.475	2.256	−1.411 to 2.361	.570
Fracture gap laterally, mm	0.788	1.470	−0.442 to 2.017	.174
Volar tilt, deg	2.588	6.659	−2.979 to 8.154	.308

Note. Data are presented as the difference between the traditional fiberglass casts and 3D-printed cast. CI = confidence interval.

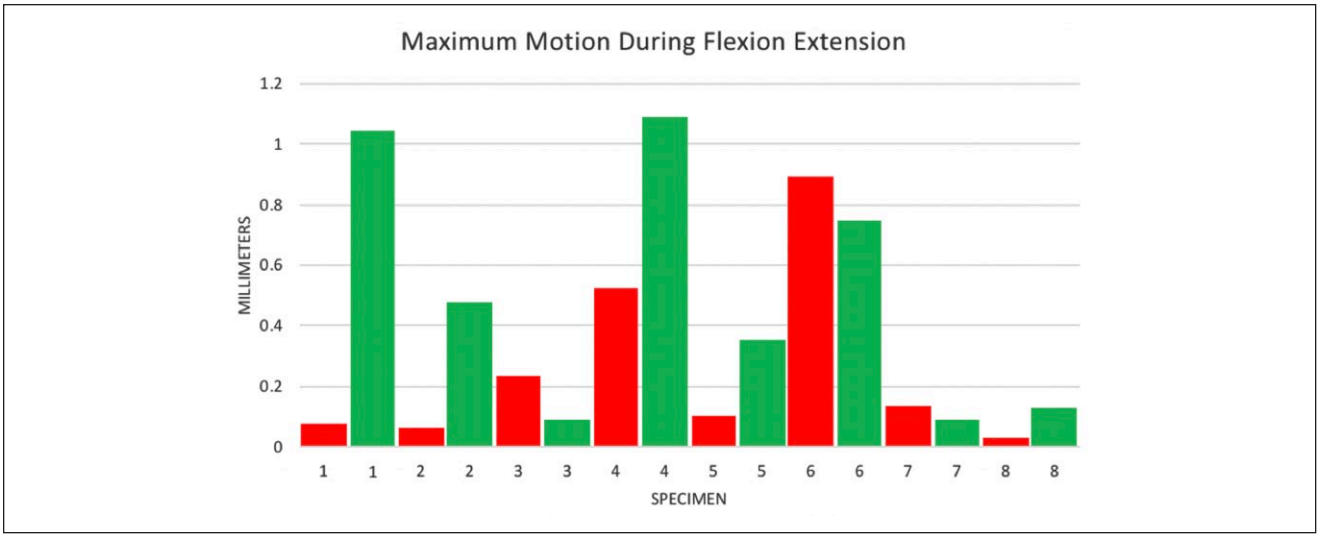

Figure 4. Maximum fracture motion during the 3 biomechanical testing modalities.
Note. Red = fiberglass cast; green = 3D-printed cast.

Table 3. Results of Biomechanical Testing and Statistical Analysis.

Modality	Mean	SD	95% CI	*P* value
Flexion-extension	−0.245	0.388	−0.570 to 0.080	.118
Pronation-supination	0.006	0.894	−0.741 to 0.754	.984
Three-point bending	−0.435	0.478	−0.834 to −0.035	.037*

Note. Data are presented as the difference between the fiberglass and 3D-printed cast groups. CI = confidence interval.
*Statistically significant.

A statistically significant difference was calculated for the 3-point bending test ($P = .037$) between the traditional fiberglass casts and the 3DPC, with a mean difference of 0.44 (±0.48) mm of motion.

Discussion

This is the first biomechanical study using a cadaveric subacute fracture model to quantify the stabilizing properties of a 3D-printed short-arm cast and to compare those properties with those of traditional fiberglass casts in a cadaveric subacute distal radius fracture model. Radiographic assessment did not reveal statistically significant differences between the 2 groups before and after biomechanical testing. The quantitative motion sensor analysis during biomechanical testing showed no statistically significant differences when comparing both immobilization techniques during the flexion-extension and pronation-supination testing. Only the 3-point bending test resulted in a statistically significant difference ($P = .037$) in motion between the specimens in a traditional fiberglass cast and those in a 3DPC. However, the clinical relevance of this motion remains unclear as the absolute motion was minimal (0.44 [±0.48] mm). Furthermore, the OptoTrak sensors were mounted on K-wires away from the osteotomies in the sagittal plane, which can cause an amplification in the measured motion. This inaccuracy

means that the ranges of motion detected by the sensor might be even smaller at the fracture site, supporting the notion that the 3DPC may be a safe alternative for immobilizing fractures of the distal radius.

In clinical practice, radiographs are used to assess displacement. This study identified consistent radiological measurements throughout the testing cycles for radial inclination, radial height, and fracture gap length on the lateral projection of the distal radius. More heterogeneous outcomes were found during measurements of the fracture gap length on the AP projection of the distal radius and during measurements of the volar tilt. The differences in measurements of the volar tilt can be attributed to image projection variability and measurement errors. Most importantly, the outcomes before and after testing are similar within each specimen pair, and the recorded heterogeneity was found to be similar in both the traditional fiberglass and 3DPC groups. Regarding the fracture gap measurements, we found more variable measurements on the AP projections. The AP image is not the ideal projection to measure fracture gap length in a dorsal wedge fracture model due to overlapping cortices. This is supported by our uniform measurement outcomes of the fracture gap length on the lateral projection which is the ideal projection for measuring this.

A subacute fracture model was chosen to reflect our institutional practice concerning nonoperative distal radius fracture treatment. At our institution, nonoperative distal radius fractures are initially treated in a sugar-tong splint for a period of 2 to 3 weeks before they are transitioned to a short-arm cast. This allows for early callus formation to withstand limited pronation and supination in a short-arm cast. There is no consensus on whether the elbow needs to be immobilized. A randomized clinical trial is currently being conducted at Johns Hopkins University to address this question (clinicaltrials.gov NCT02679066). As 3DPCs are anatomically accurate, scanning a swollen wrist in the acute setting will most likely result in a loose cast as the swelling decreases. More research needs to be conducted to assess the safety of applying 3DPCs in the acute setting.

To our knowledge, there is no prior research available on biomechanical testing of cadaveric 3DPC constructs. The strength of this study is the fact that the force magnitude applied during the cyclic loading protocols is challenging to the cast construct and most likely far exceeds the forces necessary for normal activities of daily living.

As this is a cadaveric study, our specimens were subject to all limitations native to tissue handling through freeze-thaw cycles. In particular, for the smaller cadaveric samples (1 and 6), this resulted in poorer fit of the cast with interval freeze-thaw cycles, which seems to be represented in the data via greater motion of the fracture elements. However, regardless of this, we did not find a statistically significant difference between the 2 immobilizing techniques. Another limitation is that the fracture model does not perfectly mimic the clinical scenario of a partially healed 3-week-old distal radius fracture with early callus formation. However, any imperfections were shared equally between fiberglass and 3DPC test scenarios.

This study is the first ever biomechanical testing of a novel 3DPC that shows noninferiority compared with a traditional fiberglass cast in immobilizing a subacute fracture model. The industry of 3DPCs is in its infancy, and important issues concerning costs, efficiency, and clinical results are unknown. But before these questions can be addressed, the authors believe a proper initial step in evaluating the applicability of 3DPCs is the biomechanical evaluation presented here.

The results of this study support the execution of a prospective randomized clinical trial comparing both casting techniques.

Ethical Approval

This study was approved by our institutional review board.

Statement of Human and Animal Rights

This article does not contain any studies with human or animal subjects.

Statement of Informed Consent

Informed consent was obtained when necessary.

Declaration of Conflicting Interests

The author(s) declared the following potential conflicts of interest with respect to the research, authorship, and/or publication of this article: NL reports grants and nonfinancial support from Standard Cyborg, San Francisco, California, during the conduct of the study. All other authors declare that they have no conflicts of interest.

Funding

The author(s) disclosed receipt of the following financial support for the research, authorship, and/or publication of this article: This study received financial support and materials from Standard Cyborg, San Francisco, California.

ORCID iD

Riley Knox https://orcid.org/0000-0002-4017-2363

References

1. Beerekamp MSH, de Muinck Keizer RJO, Schep NWL, et al. Epidemiology of extremity fractures in the Netherlands. *Injury*. 2017;48:1355-1362. doi:10.1016/j.injury.2017.04.047.
2. Jerrhag D, Englund M, Karlsson MK, et al. Epidemiology and time trends of distal forearm fractures in adults—a study of 11.2 million person-years in Sweden. *BMC Musculoskelet Disord*. 2017;18:240. doi:10.1186/s12891-017-1596-z.
3. Ju JH, Jin GZ, Li GX, et al. Comparison of treatment outcomes between nonsurgical and surgical treatment of distal

radius fracture in elderly: a systematic review and meta-analysis. *Langenbecks Arch Surg*. 2015;400:767-779. doi:10.1007/s00423-015-1324-9.

4. Yu GS, Lin YB, Le LS, et al. Internal fixation vs conservative treatment for displaced distal radius fractures: a meta-analysis of randomized controlled trials. *Ulus Travma Acil Cerrahi Derg*. 2016;22:233-241. doi:10.5505/tjtes.2015.05995.
5. Al Khudairy A, Hirpara KM, Kelly IP, et al. Conservative treatment of the distal radius fracture using thermoplastic splint: pilot study results. *Eur J Orthop Surg Traumatol*. 2013;23:647-650. doi:10.1007/s00590-012-1042-8.
6. Bullen M, Kinealy J, Blanchard R, et al. Comparison of the moulding ability of Plaster of Paris and polyester cast material in the healthy adult forearm. *Injury*. 2017;48:2586-2589. doi:10.1016/j.injury.2017.08.010.
7. Chen YJ, Lin H, Zhang X, et al. Application of 3D-printed and patient-specific cast for the treatment of distal radius fractures: initial experience. *3D Print Med*. 2017;3:11. doi:10.1186/s41205-017-0019-y.
8. Zhu M, Lokino ES, Chan CSH, et al. Cast immobilisation for the treatment of paediatric distal radius fracture: fibreglass versus polyolefin [published online ahead of print September 24, 2018]. *Singapore Med J*. doi:10.11622/smedj.2018118.
9. Santoni BG, Aira JR, Diaz MA, et al. Radiographic evaluation of acute distal radius fracture stability: a comparative cadaveric study between a thermo-formable bracing system and traditional fiberglass casting. *Clin Biomech (Bristol, Avon)*. 2017;47:20-26. doi:10.1016/j.clinbiomech.2017.05.009.
10. Putnam MD, Meyer NJ, Nelson EW, et al. Distal radial metaphyseal forces in an extrinsic grip model: implications for postfracture rehabilitation. *J Hand Surg Am*. 2000;25:469-475. doi:10.1053/jhsu.2000.6915.